Exploring Ultracold Collisions in ^{6}Li-^{53}Cr Fermi Mixtures: Feshbach Resonances and Scattering Properties of a Novel Alkali-Transition Metal System

A. Ciamei,[1,2,*] S. Finelli,[1,2] A. Trenkwalder,[1,2] M. Inguscio,[1,2,3] A. Simoni,[4,†] and M. Zaccanti[1,2]
[1]*Istituto Nazionale di Ottica del Consiglio Nazionale delle Ricerche (CNR-INO), 50019 Sesto Fiorentino, Italy*
[2]*European Laboratory for Non-Linear Spectroscopy (LENS), Università di Firenze, 50019 Sesto Fiorentino, Italy*
[3]*Department of Engineering, Campus Bio-Medico University of Rome, 00128 Rome, Italy*
[4]*Univ Rennes, CNRS, IPR (Institut de Physique de Rennes)-UMR 6251, F-35000 Rennes, France*

(Received 30 March 2022; revised 12 May 2022; accepted 21 July 2022; published 26 August 2022)

We investigate ultracold collisions in a novel mixture of ^{6}Li and ^{53}Cr fermionic atoms, discovering more than 50 interspecies Feshbach resonances via loss spectroscopy. Building a full coupled-channel model, we unambiguously characterize the ^{6}Li-^{53}Cr scattering properties and yield predictions for other isotopic pairs. In particular, we identify various Feshbach resonances that enable the controlled tuning of elastic s- and p-wave ^{6}Li-^{53}Cr interactions. Our studies thus make lithium-chromium mixtures emerge as optimally suited platforms for the experimental search of elusive few- and many-body regimes of highly correlated fermionic matter, and for the realization of a new class of ultracold polar molecules possessing both electric and magnetic dipole moments.

DOI: 10.1103/PhysRevLett.129.093402

Strongly interacting mixtures of two different kinds of fermionic particles [1–4] exhibit a plethora of few- and many-body phenomena extending well beyond single-component systems. In particular, this holds true for ultracold mixtures of chemically different atomic species, for which strong interactions, combined with a *heavy-light* mass imbalance M/m, are predicted to promote a variety of exotic regimes that are hard, or even impossible to attain with their homonuclear counterparts. Notable examples are exotic few-particle clusters [5–18] expected to develop for peculiar mass asymmetries $8 \lesssim M/m \lesssim 14$ [7–11], novel types of impurity physics [19–22], and mediated quasiparticle interactions [23–25], which promote the emergence of elusive many-body states [26–29]. Moreover, weakly bound bosonic dimers created from a Fermi mixture, thanks to their increased collisional stability [30,31] near an s-wave Feshbach resonance (FR) [32], represent an unparalleled starting point to realize degenerate samples of ground-state polar molecules [33–38]. This has stimulated the search for heteronuclear Fermi systems with suitable Feshbach resonances, resulting in pioneering studies of the bialkali ^{6}Li-^{40}K combination [39–47], and by a more recent investigation of ^{40}K-^{161}Dy [48] and ^{6}Li-^{173}Yb [49] alkali-lanthanide mixtures.

Here, we explore ultracold collisions in a novel ^{6}Li-^{53}Cr Fermi mixture of alkali and transition metal atoms, which is uniquely interesting for two main reasons: First, the peculiar chromium-lithium mass ratio, $M/m \sim 8.8$, is optimally suited to unveil novel non-Efimovian few-body states [7–11]. Notably, these are predicted to be collisionally stable, implying that their presence within a many-particle system will not lead to a reduced lifetime [8,28,31]. This may open the unparalleled possibility to resonantly increase [8–10] nonperturbative, *elastic* few-body effects, and to probe their impact at the many-body level. Second, recent studies [50] predict LiCr ground-state dimers to combine a large electric dipole moment exceeding 3 Debye with a $5/2$ electronic spin, making Li-Cr mixtures appealing candidates to realize ultracold polar, paramagnetic molecules. Yet, whether Li-Cr mixtures exhibit favorable scattering properties, crucial to access these compelling scenarios, has been so far unpredictable due to the complete lack of experimental input.

We positively answer this question by identifying various s- and p-wave Feshbach resonances well suited for the controlled tuning of elastic Li-Cr interactions. Through loss spectroscopy measurements [32] we reveal more than 50 isolated interspecies FRs, arranged in nonchaotic patterns despite the dipolar nature and complex level structure of fermionic ^{53}Cr [51], reminiscent of ^{161}Dy [52] and ^{167}Er [53]. We construct a full coupled-channel model [32] able to unambiguously connect the observed features to well-defined LiCr molecular states. We experimentally characterize one among such resonances, finding excellent agreement with our model predictions. We also find favorable scenarios for other isotopic pairs, opening the route to future few- and many-body studies with resonantly interacting lithium-chromium mixtures.

By following procedures reported elsewhere [51,54], we produce ultracold samples of ^{6}Li and ^{53}Cr atoms in a bichromatic optical dipole trap (BODT), formed by a multimode infrared (IR) laser beam centered at 1073 nm [55], overlapped with a green beam at 532 nm, focused to a waist of 45 μm and 40 μm, respectively. The lithium-to-chromium trap depth ratio set by the primary IR source,

 © 2022 American Physical Society

of about 3, can be reduced by the green light, which confines chromium and anticonfines lithium, allowing one to controllably adjust the Li and Cr populations, densities, and temperature. To perform FR scans, we employ ultracold mixtures at $10(1)$ μK, trapped in the sole IR beam with negligible differential gravitational sag, comprising about 10^5 Cr and 1.8×10^6 Li atoms, characterized by Cr (Li) peak densities of 10^{11} cm^{-3} (2×10^{12} cm^{-3}).

Spin-state manipulation [54] allows us to explore different binary Li-Cr mixtures: lithium is prepared in either of the two lowest Zeeman levels of the electronic and hyperfine ground-state manifold $^2S_{1/2}$, $|f_{\mathrm{Li}} = 1/2, m_{f,\mathrm{Li}} = \pm 1/2\rangle$, hereafter labeled Li$|1\rangle$ and Li$|2\rangle$, respectively [56]. Chromium, initially produced in the lowest hyperfine and Zeeman level $|f_{\mathrm{Cr}} = 9/2, m_{f,\mathrm{Cr}} = -9/2\rangle$ of its electronic ground state $^7S_3$ [51] (hereafter denoted Cr$|1\rangle$), can also be transferred to the two higher-lying Zeeman states of the $f_{\mathrm{Cr}} = 9/2$ manifold, labeled Cr$|2\rangle$ and Cr$|3\rangle$, respectively. We explore all six Li$|i\rangle$-Cr$|j\rangle$ mixtures with $i = 1$, 2 and $j = 1$, 2, 3, each being characterized by the total spin projection quantum number, $M_f = m_{f,\mathrm{Li}} + m_{f,\mathrm{Cr}} = -i + j - 4$, thus spanning $-5 \leq M_f \leq -2$.

We perform loss spectroscopy through magnetic-field scans with typical step size of 60 mG. We keep the sample at a variable field for a fixed time t_H, and then monitor the remaining atoms via spin-selective absorption imaging [54]. FRs are identified by enhanced atom losses, induced by different processes depending on the spin combination investigated [32]. Any Li$|i\rangle$-Cr$|j\rangle$ mixture but the lowest-energy one, $i = j = 1$, may undergo two-body losses. Inelastic spin exchange occurs whenever the initial atom pair is coupled to an energetically lower channel with equal M_f and orbital partial wave l. Such a process does not affect excited spin combinations with either Li or Cr in the ground state (i or $j = 1$). Weaker dipolar relaxation processes are enabled by spin-dipole coupling [32] for any excited mixture, that can decay to lower-lying states with different M_f or l, provided that $\Delta l = 0, \pm 2$ and $M_f + m_l$ is conserved, m_l being the projection of l along the magnetic-field quantization axis [42]. Three-body recombination processes affect any mixture. While these can in principle involve either two light and one heavy atom or vice versa, only the former case is relevant here, given our Li-Cr density imbalance.

Figure 1 provides an overview of FR scans for four of the six Li-Cr combinations explored herein, from which important insights can be gained. None of the mixtures exhibits a dense FR spectrum, in contrast with mixtures of alkalis and Er or Dy lanthanides [48,57]. Similarly to bialkali systems, see e.g., Ref. [39], none of the loss peaks is due to, or overlapped with, Cr-Cr or Li-Li resonances. Additionally, nearly coincident FR locations found among different spectra, both for mixtures with equal M_f values [see Figs. 1(b) and 1(c)], and unequal ones, suggest that relatively few molecular states, split into different hyperfine

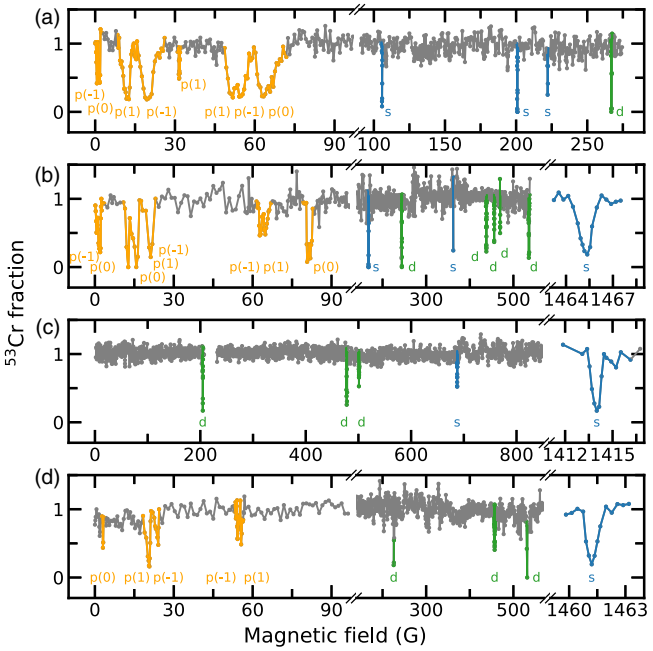

FIG. 1. Overview of ^{6}Li-^{53}Cr loss spectra. The remaining Cr number, normalized to its background value, recorded after an interaction time t_H with lithium, is plotted as a function of the magnetic field for four different combinations: (a) Li$|2\rangle$-Cr$|3\rangle$, $M_f = -3$; (b) Li$|2\rangle$-Cr$|2\rangle$, $M_f = -4$; (c) Li$|1\rangle$-Cr$|1\rangle$, $M_f = -4$; and (d) Li$|2\rangle$-Cr$|1\rangle$, $M_f = -5$. Each point is the average of at least four independent measurements. $t_H = 4$ s for all but the (c) panel, where $t_H = 5$ s. Features that our model links to s-, p- and d-wave molecular levels are colored blue, orange, and green, respectively. Numbers in brackets indicate the assigned m_l.

levels, suffice to explain our observation. Finally, while few, sparse, and narrow features characterize the high-field spectral regions above 150 G, each scan but the Li$|1\rangle$-Cr$|1\rangle$ one exhibits more complex patterns below 150 G, with strong loss peaks arranged in doublet or triplet structures; see, e.g., Fig. 1(b). This suggests that three-body losses are overcome by two-body ones in such a field region, and that the observed FRs likely occur in $l > 0$ partial waves, split by the magnetic dipole-dipole interaction [58,59] and possibly other couplings [60].

This intuition is supported by additional loss data, recorded near two low-field Li$|2\rangle$-Cr$|1\rangle$ FRs on low-density samples that were prepared at 5 μK and 24 μK, shown in Figs. 2(a) and 2(b), respectively. Both features are highly asymmetric, and they sensitively widen for increasing temperature, a behavior typical of $l > 0$-wave FRs [58,59,61]. Without aiming at a quantitative line shape analysis, we remark that our data are well reproduced (see solid lines in Fig. 2) by a simple model [62] that assumes $l = 1$ collisions and solely accounts for two-body processes [63]. Another peculiarity of Fig. 2 spectra, common to other features in Fig. 1, is their thermal tail [58,59,61] oriented toward lower fields. This implies that such FRs originate from "anomalous" molecular levels that

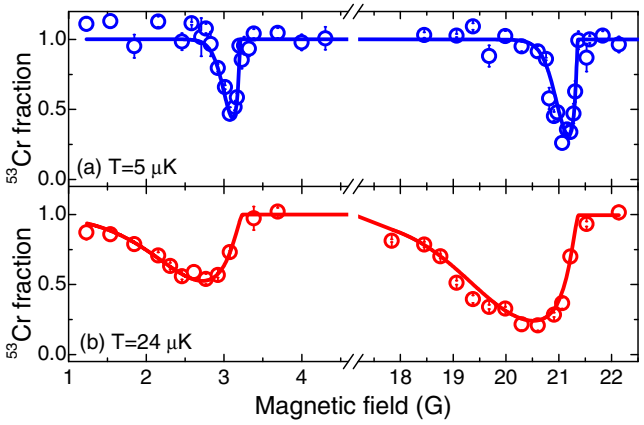

FIG. 2. Temperature dependence of atom loss at two low-field FRs of Li$|2\rangle$-Cr$|1\rangle$. (a) The remaining Cr fraction, recorded after $t_H = 4$ s with a Li sample at 5 μK, is plotted as a function of the magnetic field. (b) Same as (a) but for 24 μK. Each data point is the average of three independent measurements. Lines are best fits to the model of Ref. [62] for p-wave collisions.

lay slightly above the atomic threshold at zero field and cross it with negative differential magnetic moments.

We now move to quantitatively analyze our spectroscopic data building a full coupled-channel model [32]. This accounts for the atomic hyperfine and Zeeman energies [64,65], defining the asymptotic collision thresholds. The electrostatic interaction is represented by adiabatic Born-Oppenheimer potentials of *sextet* $X^6\Sigma^+$ and *octet* $a^8\Sigma^+$ symmetry, where $S = 5/2$ and $7/2$ denote the total electron spin of LiCr dimers. Such potentials, correlating at long range with the well-known analytical form [32] comprising a multipolar expansion plus the exchange potential, are parametrized in terms of sextet a_6 and octet a_8 s-wave scattering lengths, respectively. Besides this strong isotropic interaction, both l and M_f conserving, we also account for weaker anisotropic couplings originating from the long-range magnetic spin and short-range second-order spin-orbit interactions. These terms can couple different partial waves and hyperfine states, with the selection rules discussed above for dipolar relaxation processes [32,66].

Starting from the *ab initio* data and long-range potential parameters of Ref. [76], we optimize the initially unknown values of a_6 and a_8, and of the dispersion coefficients C_6 and C_8, using least-square iterations by comparison with the experimental data. By tentatively identifying the isolated loss peaks above 1 kG as spin-exchange s-wave FRs associated with $S = 5/2$ rotationless ($l_r = 0$) molecular states, the sextet scattering length is strongly constrained to $a_6 = 15.5a_0$. This also reproduces several other features at lower field, assigned to $l_r = 2$ states of the $S = 5/2$ potential, thus confirming the hypothesis. A strong constraint on a_8 is instead provided by the peculiar low-field patterns, characterized by irregularly spaced triplets and several "anomalous" FRs (see Fig. 2). A global least-square fit to the observed FRs yields the best-fit parameters $a_6 = 15.46(15)a_0$, $a_8 = 41.48(2)a_0$, $C_6 = 922(6)$ a.u., and $C_8 = 9.8(5) \times 10^4$ a.u., where errors represent one standard deviation obtained from the fit covariance matrix. We remark that our a_8 value agrees well with recent *ab initio* estimates [50].

TABLE I. Selection of ^{6}Li-^{53}Cr Feshbach resonances immune to inelastic spin-exchange decay. Experimental $B_{\rm exp}$ and theoretical B_0 locations are compared for Li-Cr (i, j) channels. $B_{\rm exp}$ are obtained from the zeroes of the numerically computed first derivative of loss data. A conservative 200 mG uncertainty combines our 10 mG field stability over 4 s with day-by-day field drift and systematic errors. For incoming s-wave (p-wave) FRs, background scattering lengths $a_{\rm bg}^{(0)}$ (volumes $a_{\rm bg}^{(1)}$) and magnetic widths $\Delta_{\rm el}$ are computed in the zero-energy limit (at collision energy $E/k_B = 10$ μK). Coupled s and d waves (p wave only) are included for s-wave (p-wave) resonances. The differential magnetic moment $\delta\mu$, the electron spin S_r, and the rotational angular momentum l_r of the molecular state are also listed. Additional data are reported in the Supplemental Material [66].

i, j, l, m_l	$B_{\rm exp}$ (G)	B_0 (G)	S_r, l_r	$a_{\rm bg}^{(l)}$ (a_0^{2l+1})	$\Delta_{\rm el}$ (G)	$\delta\mu$ (μ_B)
1,1,0,0	204.6	204.7	5/2, 2	41.3	7.0×10^{-3}	3.7
1,1,0,0	477.6	478.1	5/2, 2	41.5	1.8×10^{-3}	2.0
1,1,0,0	501.0	501.9	5/2, 2	41.5	3.8×10^{-4}	2.0
1,1,0,0	687.4	687.1	5/2, 0	41.5	2.3×10^{-4}	4.0
1,1,0,0	1414.0	1414.1	5/2, 0	41.5	0.47	2.0
2,1,1,0	3.05	2.3	7/2, 1	-1.6×10^5	−3.70	−0.56
2,1,1,1	21.1	20.9	7/2, 1	8.2×10^3	119	−0.28
2, 1, 1, −1	24.2	24.2	7/2, 1	2.5×10^4	37.8	−0.24
2, 1, 1, −1	54.3	54.8	7/2, 1	1.4×10^5	−4.56	0.27
2,1,1,1	55.6	56.1	7/2, 1	-1.1×10^5	5.08	0.31
2,1,0,0	225.7	225.8	5/2, 2	41.3	7.4×10^{-3}	3.8
2,1,0,0	457.0	456.7	5/2, 2	41.5	3.6×10^{-4}	2.0
2,1,0,0	531.4	531.8	5/2, 2	41.5	2.3×10^{-4}	2.0
2,1,0,0	1461.2	1461.2	5/2, 0	41.5	0.48	2.0
1,2,0,0	65.0	65.9	7/2, 0	39.5	6.6×10^{-3}	3.1
1,2,0,0	135.7	135.7	5/2, 2	40.8	3.7×10^{-5}	5.0
1,2,0,0	139.5	140.4	7/2, 0	40.8	1.9×10^{-3}	3.0
1,2,0,0	483.5	484.2	5/2, 2	41.5	1.7×10^{-2}	2.0
1,2,0,0	1418.1	1417.9	5/2, 0	41.5	0.47	2.0

Our quantum collisional model accurately reproduces the experimental findings, as shown in Table I for a subset of 20 FRs. Besides the magnetic field location, we provide the relevant quantum numbers for both the entrance channel and molecular state, together with the associated resonance parameters: background scattering length $a_{\rm bg}^{(0)}$ (or volume $a_{\rm bg}^{(1)}$), magnetic width $\Delta_{\rm el}$, and magnetic moment $\delta\mu$ of the molecular state relative to the atomic threshold. The low-field spectral region is entirely dominated by p-wave FRs, featuring m_l splittings much larger than those found in alkali systems [58–60], owing to the increased role of spin-spin dipole coupling in Li-Cr mixtures and to the coincidentally small relative magnetic

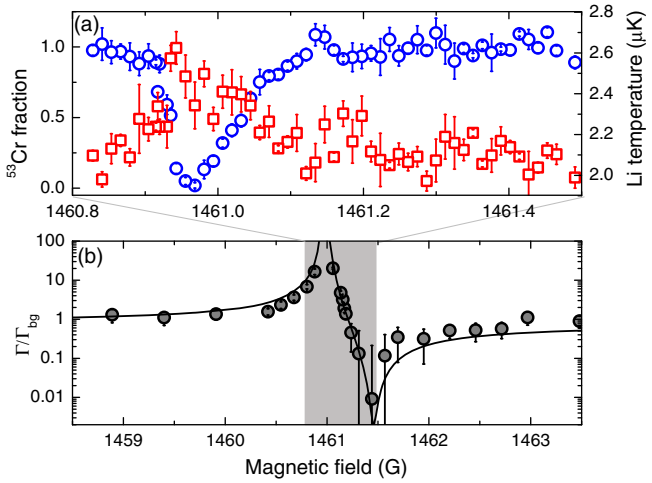

FIG. 3. Inelastic and elastic scattering at a Li$|2\rangle$-Cr$|1\rangle$ s-wave FR. (a) Magnetic-field dependence of the remaining Cr fraction (blue circles, left axis) and final Li temperature (red squares, right axis), recorded on a mixture at 2 μK after 150 ms interaction time. Each data point is the average of at least three independent measurements. The loss peak corresponds to a $1/e$ lifetime of 40(3) ms. (b) Field dependence of the collision-induced damping rate Γ of a Li cloud at 2 μK, sloshing along the weak axis of the BODT in the presence of a Cr cloud at rest. Experimentally determined normalized $\Gamma/\Gamma_{\rm bg}$ is compared with the thermally averaged elastic scattering rate given by our model (solid line). Error bars account for the statistical error of the fit of the oscillation data to a damped sinusoidal function. The shaded area marks panel (a) boundaries. For both panels the field uncertainty is 5 mG.

moment of the molecular states involved. In particular, we highlight the presence in Li$|2\rangle$-Cr$|1\rangle$ of a strong p-wave FR with $m_l = -1$, centered around 24 G and essentially immune to two-body losses [66], well-suited to investigate p-wave resonant Fermi mixtures [77].

We also identify various s-wave FRs in different spin combinations, including the absolute Li-Cr ground state. Owing to the relatively small values of a_6 and a_8 [32], similar to the Li-K case [39,42], these features are generally narrow. In particular, our model connects all FRs above 1400 G to $l_r = 0$ molecular levels of $X^6\Sigma^+$ potentials, predicting negligible two-body loss rates, magnetic-field widths $\Delta_{\rm el} \sim 0.5$ G, and associated effective-range parameters [32,44] of a few 1000 a_0.

We test these expectations by inspecting inelastic and elastic properties of the FR located at 1461 G occurring in the Li$|2\rangle$-Cr$|1\rangle$ channel. Figure 3(a) shows a 10 mG-resolution loss scan, performed with a mixture initially produced at 2 μK, comprising about 5×10^5 Li and 10^5 Cr atoms, respectively, and characterized by a Li (Cr) peak density of about 4×10^{12} cm^{-3} (10^{12} cm^{-3}). Through a 30 ms-long linear ramp, the magnetic field is lowered from 1464 G to the final value, where the sample is held for 150 ms. The observed loss feature, shown in Fig. 3(a) for the Cr component (blue circles), is strongly asymmetric, as expected for narrow FRs [78]. Contrary to the low-field FRs of Fig. 2, here we find a lithium-to-chromium loss ratio consistent with 2 within experimental uncertainty. This points to Li-Li-Cr three-body processes that overcome two-body ones, in agreement with our model expectation of a small dipolar relaxation rate $K_2 < 10^{-14}$ cm^3/s at 2 μK. Concurrently, we observe a sizable temperature increase of the Li cloud [red squares in Fig. 3(a)], pointing to antievaporation dynamics due to recombination processes [32].

Additionally, we investigate the magnetic-field dependence of the Li-Cr elastic scattering across this FR. By means of experimental protocols identical to those of Ref. [42], we monitor the damping of the sloshing motion of a lithium cloud of about 5×10^4 atoms, along the weak axis of our BODT, induced by interspecies collisions with about 10^5 Cr atoms prepared at 2 μK [54]. A species-selective optical excitation [42] initiates sloshing of the Li component while negligibly affecting the Cr one. For each field, we trace the Li center-of-mass oscillations, which are fit to a damped sinusoidal function to extract the damping rate Γ. For weak interactions, with only few scattering events per oscillation period, Γ is directly proportional to the elastic scattering rate [42]. Figure 3(b) shows the experimentally determined Γ, normalized to the background value $\Gamma_{\rm bg}$ measured far from the resonant region (circles), together with the thermally averaged elastic scattering rate obtained from our collisional model (solid line). The remarkable agreement between experimental and theoretical data further demonstrates the accuracy of our theory, confirming the model expectation of $\Delta_{\rm el} \sim 0.5$ G.

Finally, we exploit our quantum collisional model to inspect the scattering properties of other isotopic pairs. Specifically, we focus on the Fermi-Bose mixtures ^{6}Li-^{52}Cr and ^{7}Li-^{53}Cr, obtained by replacing fermionic Cr and Li with their most abundant bosonic isotopes, respectively. Within the Born-Oppenheimer approximation, this can be achieved by simply changing the reduced mass in the Hamiltonian, although the result depends upon the actual number of vibrational states N_6 and N_8 of the sextet and octet potentials, which bear an uncertainty of a few units [66]. Setting them to the nominal values employed in our fit [76], for the ^{6}Li-^{52}Cr combination we obtain $a_6^{6-52} = 19.88(13)a_0$ and $a_8^{6-52} = 42.83(2)a_0$, finding a few ~100 mG-wide resonances at fields of a few hundred Gauss. Since the reduced mass and, correspondingly, the potential parameters of such an isotopic pair are very similar to the ^{6}Li-^{53}Cr ones, our predictions are only weakly affected by the actual N_6 and N_8 values [66]. The same procedure, applied to ^{7}Li-^{53}Cr, yields $a_6^{7-53} = 38.20(14)a_0$ and $a_8^{7-53} = 51.53(3)a_0$, respectively. Thanks to the complex hyperfine structure of ^{53}Cr, this isotopic pair exhibits richer FR spectra, and a few-Gauss-wide resonances below 500 G, although the increased sensitivity of the mass-scaled

parameters of ^{7}Li-^{53}Cr upon $N_{6,8}$ variations enhances our systematic uncertainty [66].

In conclusion, we thoroughly investigated the collisional properties of a novel ^{6}Li-^{53}Cr ultracold Fermi mixture. All Li-Cr isotopic pairs, characterized by isolated and nonchaotic FRs linked to molecular states with well-defined quantum numbers, combine the simplicity of bialkali systems with richer molecular structures as those of alkali-lanthanide or alkali-alkaline-earth mixtures [48,49,57,79]. Several strong and isolated features, already identified, with widths exceeding a few 100 mG, provide an optimal starting point to form (bosonic or fermionic) Feshbach dimers. These could be then transferred via coherent optical schemes to the ground states of the $X^6\Sigma^+$ and $a^8\Sigma^+$ potentials, both predicted [50] to feature sizable electric and magnetic dipole moments, thus making Li-Cr a competing system to realize ultracold paramagnetic polar molecules. The s-wave FRs in ^{6}Li-^{53}Cr (and ^{7}Li-^{53}Cr), with character similar to Li-K ones [39,42] but immune to two-body losses, together with an increased mass ratio, provide an unparalleled opportunity to investigate novel non-Efimovian few-body physics [9–13]. The presence of s- and p-wave FRs, featuring lifetimes of several tens of ms in the resonant region, makes lithium-chromium promising also for future many-body studies.

We thank D. Petrov, J. Szczepkowski, E. Tiemann, M. Tomza, K. Zaremba-Kopczyk, and the LENS Quantum Gases group for fruitful discussions, and G. Modugno for useful suggestions and a critical reading of the manuscript. This work was supported by the European Research Council under Grant No. 637738 (PoLiChroM), by the Italian MIUR through the FARE Grant No. R168HMHFYM (P-HeLiCS), and by the EU's Horizon 2020 research and innovation programme under the Marie Skłodowska-Curie Grant No. 894442 (CriLiN) [fellowship to A. C.].

*ciamei@lens.unifi.it
†andrea.simoni@univ-rennes1.fr

[1] R. Casalbuoni and G. Nardulli, Inhomogeneous superconductivity in condensed matter and QCD, Rev. Mod. Phys. **76**, 263 (2004).
[2] H.-W. Hammer, A. Nogga, and A. Schwenk, Colloquium: Three-body forces: From cold atoms to nuclei, Rev. Mod. Phys. **85**, 197 (2013).
[3] G. Wang, A. Chernikov, M. M. Glazov, T. F. Heinz, X. Marie, T. Amand, and B. Urbaszek, Colloquium: Excitons in atomically thin transition metal dichalcogenides, Rev. Mod. Phys. **90**, 021001 (2018).
[4] Y. Jiang, S. Chen, W. Zheng, B. Zheng, and A. Pan, Interlayer exciton formation, relaxation, and transport in TMD van der Waals heterostructures, Light Sci. Appl. **10**, 72 (2021).
[5] V. Efimov, Energy levels of three resonantly interacting particles, Nucl. Phys. **A210**, 157 (1973).
[6] Y. Castin, C. Mora, and L. Pricoupenko, Four-Body Efimov Effect for Three Fermions and a Lighter Particle, Phys. Rev. Lett. **105**, 223201 (2010).
[7] S. Endo, P. Naidon, and M. Ueda, Universal physics of $2+1$ particles with non-zero angular momentum, Few-Body Syst. **51**, 207 (2011).
[8] J. Levinsen and D. S. Petrov, Atom-dimer and dimer-dimer scattering in fermionic mixtures near a narrow Feshbach resonance, Eur. Phys. J. D **65**, 67 (2011).
[9] S. Endo, P. Naidon, and M. Ueda, Crossover trimers connecting continuous and discrete scaling regimes, Phys. Rev. A **86**, 062703 (2012).
[10] B. Bazak and D. S. Petrov, Five-Body Efimov Effect and Universal Pentamer in Fermionic Mixtures, Phys. Rev. Lett. **118**, 083002 (2017).
[11] O. I. Kartavtsev and A. V. Malykh, Low-energy three-body dynamics in binary quantum gases, J. Phys. B **40**, 1429 (2007).
[12] Y. Nishida and S. Tan, Universal Fermi Gases in Mixed Dimensions, Phys. Rev. Lett. **101**, 170401 (2008).
[13] J. Levinsen, T. G. Tiecke, J. T. M. Walraven, and D. S. Petrov, Atom-Dimer Scattering and Long-Lived Trimers in Fermionic Mixtures, Phys. Rev. Lett. **103**, 153202 (2009).
[14] V. Ngampruetikorn, M. M. Parish, and J. Levinsen, Three-body problem in a two-dimensional Fermi gas, Europhys. Lett. **102**, 13001 (2013).
[15] J. Levinsen and M. M. Parish, Bound States in a Quasi-Two-Dimensional Fermi Gas, Phys. Rev. Lett. **110**, 055304 (2013).
[16] D. Blume, Few-body physics with ultracold atomic and molecular systems in traps, Rep. Prog. Phys. **75**, 046401 (2012).
[17] B. Bazak, Mass-imbalanced fermionic mixture in a harmonic trap, Phys. Rev. A **96**, 022708 (2017).
[18] R. Liu, C. Peng, and X. Cui, Universal tetramer and pentamer in two-dimensional fermionic mixtures, arXiv:2202.01437.
[19] C. J. M. Mathy, M. M. Parish, and D. A. Huse, Trimers, Molecules, and Polarons in Mass-Imbalanced Atomic Fermi Gases, Phys. Rev. Lett. **106**, 166404 (2011).
[20] P. Massignan, M. Zaccanti, and G. M. Bruun, Polarons, dressed molecules and itinerant ferromagnetism in ultracold Fermi gases, Rep. Prog. Phys. **77**, 034401 (2014).
[21] R. Schmidt, M. Knap, D. A. Ivanov, J.-S. You, M. Cetina, and E. Demler, Universal many-body response of heavy impurities coupled to a Fermi sea: A review of recent progress, Rep. Prog. Phys. **81**, 024401 (2018).
[22] R. Liu, C. Peng, and X. Cui, Crystalline correlations emergent from a smooth crossover of mass-imbalanced Fermi polaron, arXiv:2202.03623.
[23] A. Bulgac, M. M. Forbes, and A. Schwenk, Induced p-Wave Superfluidity in Asymmetric Fermi Gases, Phys. Rev. Lett. **97**, 020402 (2006).
[24] D. Suchet, Z. Wu, F. Chevy, and G. M. Bruun, Long-range mediated interactions in a mixed-dimensional system, Phys. Rev. A **95**, 043643 (2017).
[25] A. Camacho-Guardian and G. M. Bruun, Landau Effective Interaction between Quasiparticles in a Bose-Einstein Condensate, Phys. Rev. X **8**, 031042 (2018).

[26] K. B. Gubbels, J. E. Baarsma, and H. T. C. Stoof, Lifshitz Point in the Phase Diagram of Resonantly Interacting ^{6}Li-^{40}K Mixtures, Phys. Rev. Lett. **103**, 195301 (2009).

[27] K. Gubbels and H. Stoof, Imbalanced Fermi gases at unitarity, Phys. Rep. **525**, 255 (2013).

[28] S. Endo, A. M. García-García, and P. Naidon, Universal clusters as building blocks of stable quantum matter, Phys. Rev. A **93**, 053611 (2016).

[29] M. Pini, P. Pieri, R. Grimm, and G. C. Strinati, Beyond-mean-field description of a trapped unitary Fermi gas with mass and population imbalance, Phys. Rev. A **103**, 023314 (2021).

[30] D. S. Petrov, C. Salomon, and G. V. Shlyapnikov, Weakly Bound Dimers of Fermionic Atoms, Phys. Rev. Lett. **93**, 090404 (2004).

[31] M. Jag, M. Cetina, R. S. Lous, R. Grimm, J. Levinsen, and D. S. Petrov, Lifetime of Feshbach dimers in a Fermi-Fermi mixture of ^{6}Li and ^{40}K, Phys. Rev. A **94**, 062706 (2016).

[32] C. Chin, R. Grimm, P. Julienne, and E. Tiesinga, Feshbach resonances in ultracold gases, Rev. Mod. Phys. **82**, 1225 (2010).

[33] K.-K. Ni, S. Ospelkaus, M. H. G. de Miranda, A. Pe'er, B. Neyenhuis, J. J. Zirbel, S. Kotochigova, P. S. Julienne, D. S. Jin, and J. Ye, A high phase-space-density gas of polar molecules, Science **322**, 231 (2008).

[34] T. Takekoshi, L. Reichsöllner, A. Schindewolf, J. M. Hutson, C. R. Le Sueur, O. Dulieu, F. Ferlaino, R. Grimm, and H.-C. Nägerl, Ultracold Dense Samples of Dipolar RbCs Molecules in the Rovibrational and Hyperfine Ground State, Phys. Rev. Lett. **113**, 205301 (2014).

[35] P. K. Molony, P. D. Gregory, Z. Ji, B. Lu, M. P. Köppinger, C. R. Le Sueur, C. L. Blackley, J. M. Hutson, and S. L. Cornish, Creation of Ultracold ^{87}Rb^{133}Cs Molecules in the Rovibrational Ground State, Phys. Rev. Lett. **113**, 255301 (2014).

[36] J. W. Park, S. A. Will, and M. W. Zwierlein, Ultracold Dipolar Gas of Fermionic ^{23}Na^{40}K Molecules in their Absolute Ground State, Phys. Rev. Lett. **114**, 205302 (2015).

[37] M. Guo, B. Zhu, B. Lu, X. Ye, F. Wang, R. Vexiau, N. Bouloufa-Maafa, G. Quéméner, O. Dulieu, and D. Wang, Creation of an Ultracold Gas of Ground-State Dipolar ^{23}Na^{87}Rb Molecules, Phys. Rev. Lett. **116**, 205303 (2016).

[38] H. Son, J. J. Park, W. Ketterle, and A. O. Jamison, Collisional cooling of ultracold molecules, Nature (London) **580**, 197 (2020).

[39] E. Wille, F. M. Spiegelhalder, G. Kerner, D. Naik, A. Trenkwalder, G. Hendl, F. Schreck, R. Grimm, T. G. Tiecke, J. T. M. Walraven, S. J. J. M. F. Kokkelmans, E. Tiesinga, and P. S. Julienne, Exploring an Ultracold Fermi-Fermi Mixture: Interspecies Feshbach Resonances and Scattering Properties of ^{6}Li and ^{40}K, Phys. Rev. Lett. **100**, 053201 (2008).

[40] A.-C. Voigt, M. Taglieber, L. Costa, T. Aoki, W. Wieser, T. W. Hänsch, and K. Dieckmann, Ultracold Heteronuclear Fermi-Fermi Molecules, Phys. Rev. Lett. **102**, 020405 (2009).

[41] L. Costa, J. Brachmann, A.-C. Voigt, C. Hahn, M. Taglieber, T. W. Hänsch, and K. Dieckmann, *s*-Wave Interaction in a Two-Species Fermi-Fermi Mixture at a Narrow Feshbach Resonance, Phys. Rev. Lett. **105**, 123201 (2010).

[42] D. Naik, A. Trenkwalder, C. Kohstall, F. M. Spiegelhalder, M. Zaccanti, G. Hendl, F. Schreck, R. Grimm, T. M. Hanna, and P. S. Julienne, Feshbach resonances in the ^{6}Li-^{40}K Fermi-Fermi mixture: Elastic versus inelastic interactions, Eur. Phys. J. D **65**, 55 (2011).

[43] A. Trenkwalder, C. Kohstall, M. Zaccanti, D. Naik, A. I. Sidorov, F. Schreck, and R. Grimm, Hydrodynamic Expansion of a Strongly Interacting Fermi-Fermi Mixture, Phys. Rev. Lett. **106**, 115304 (2011).

[44] C. Kohstall, M. Zaccanti, M. Jag, A. Trenkwalder, P. Massignan, G. M. Bruun, F. Schreck, and R. Grimm, Metastability and coherence of repulsive polarons in a strongly interacting Fermi mixture, Nature (London) **485**, 615 (2012).

[45] M. Jag, M. Zaccanti, M. Cetina, R. S. Lous, F. Schreck, R. Grimm, D. S. Petrov, and J. Levinsen, Observation of a Strong Atom-Dimer Attraction in a Mass-Imbalanced Fermi-Fermi Mixture, Phys. Rev. Lett. **112**, 075302 (2014).

[46] M. Cetina, M. Jag, R. S. Lous, J. T. M. Walraven, R. Grimm, R. S. Christensen, and G. M. Bruun, Decoherence of Impurities in a Fermi Sea of Ultracold Atoms, Phys. Rev. Lett. **115**, 135302 (2015).

[47] M. Cetina, M. Jag, R. S. Lous, I. Fritsche, J. T. M. Walraven, R. Grimm, J. Levinsen, M. M. Parish, R. Schmidt, M. Knap, and E. Demler, Ultrafast many-body interferometry of impurities coupled to a Fermi sea, Science **354**, 96 (2016).

[48] C. Ravensbergen, E. Soave, V. Corre, M. Kreyer, B. Huang, E. Kirilov, and R. Grimm, Resonantly Interacting Fermi-Fermi Mixture of ^{161}Dy and ^{40}K, Phys. Rev. Lett. **124**, 203402 (2020).

[49] A. Green, H. Li, J. H. See Toh, X. Tang, K. C. McCormick, M. Li, E. Tiesinga, S. Kotochigova, and S. Gupta, Feshbach Resonances in *p*-Wave Three-Body Recombination within Fermi-Fermi Mixtures of Open-Shell ^{6}Li and Closed-Shell ^{173}Yb Atoms, Phys. Rev. X **10**, 031037 (2020).

[50] K. Zaremba-Kopczyk, M. Gronowski, and M. Tomza, Ultracold mixtures of Cr and Li atoms: Theoretical prospects for controlled atomic collisions, LiCr molecule formation, and molecular precision measurements (to be published).

[51] E. Neri, A. Ciamei, C. Simonelli, I. Goti, M. Inguscio, A. Trenkwalder, and M. Zaccanti, Realization of a cold mixture of fermionic chromium and lithium atoms, Phys. Rev. A **101**, 063602 (2020).

[52] M. Lu, N. Q. Burdick, and B. L. Lev, Quantum Degenerate Dipolar Fermi Gas, Phys. Rev. Lett. **108**, 215301 (2012).

[53] K. Aikawa, A. Frisch, M. Mark, S. Baier, R. Grimm, and F. Ferlaino, Reaching Fermi Degeneracy via Universal Dipolar Scattering, Phys. Rev. Lett. **112**, 010404 (2014).

[54] A. Ciamei *et al.*, Double-degenerate Fermi mixtures of ^{6}Li and ^{53}Cr atoms, arXiv:2207.07579.

[55] C. Simonelli, E. Neri, A. Ciamei, I. Goti, M. Inguscio, A. Trenkwalder, and M. Zaccanti, Realization of a high power optical trapping setup free from thermal lensing effects, Opt. Express **27**, 27215 (2019).

[56] With $m_{f,a}$ we denote the projection quantum number for element $a = $ Li, Cr.

[57] F. Schäfer, N. Mizukami, and Y. Takahashi, Feshbach resonances of large-mass-imbalance Er-Li mixtures, Phys. Rev. A **105**, 012816 (2022).
[58] C. Ticknor, C. A. Regal, D. S. Jin, and J. L. Bohn, Multiplet structure of Feshbach resonances in nonzero partial waves, Phys. Rev. A **69**, 042712 (2004).
[59] Y. Cui, C. Shen, M. Deng, S. Dong, C. Chen, R. Lü, B. Gao, M. K. Tey, and L. You, Observation of Broad d-Wave Feshbach Resonances with a Triplet Structure, Phys. Rev. Lett. **119**, 203402 (2017).
[60] B. Zhu, S. Häfner, B. Tran, M. Gerken, J. Ulmanis, E. Tiemann, and M. Weidemüller, Spin-rotation coupling in p-wave Feshbach resonances, arXiv:1910.12011.
[61] L. Fouché, A. Boissé, G. Berthet, S. Lepoutre, A. Simoni, and T. Bourdel, Quantitative analysis of losses close to a d-wave open-channel Feshbach resonance in ^{39}K, Phys. Rev. A **99**, 022701 (2019).
[62] K. M. Jones, P. D. Lett, E. Tiesinga, and P. S. Julienne, Fitting line shapes in photoassociation spectroscopy of ultracold atoms: A useful approximation, Phys. Rev. A **61**, 012501 (1999).
[63] Each data set is fitted assuming exponential decay of the Cr fraction with loss rate $\gamma(B) = n_{Li}K_2(B) \equiv A(B_0 - B)^{l+1/2}\mathrm{Exp}\{-[\delta\mu(B_0 - B)/k_BT]\}$. Temperature T is fixed to the experimental value and $l = 1$. Amplitude A, FR center B_0, and magnetic moment $\delta\mu$ are fitting parameters.
[64] W. J. Childs, L. S. Goodman, and D. von Ehrenstein, Magnetic hyperfine interaction of ^{53}Cr, Phys. Rev. **132**, 2128 (1963).
[65] E. Arimondo, M. Inguscio, and P. Violino, Experimental determinations of the hyperfine structure in the alkali atoms, Rev. Mod. Phys. **49**, 31 (1977).
[66] See Supplemental Material at http://link.aps.org/supplemental/10.1103/PhysRevLett.129.093402, which includes Refs. [67–75], for further details about theory model, extraction of resonance parameters, additional theory-experiment comparison, and prediction of scattering properties of other isotopic pairs.
[67] A. Simoni, Fitting ultracold resonances without a fit, New J. Phys. **23**, 113023 (2021).
[68] J. M. Hutson, Feshbach resonances in ultracold atomic and molecular collisions: Threshold behaviour and suppression of poles in scattering lengths, New J. Phys. **9**, 152 (2007).
[69] H. R. Sadeghpour, J. L. Bohn, M. J. Cavagnero, B. D. Esry, I. I. Fabrikant, J. H. Macek, and A. R. P. Rau, Collisions near threshold in atomic and molecular physics, J. Phys. B **33**, R93 (2000).
[70] A. Derevianko, Anisotropic pseudopotential for polarized dilute quantum gases, Phys. Rev. A **67**, 033607 (2003).
[71] A. Viel and A. Simoni, Feshbach resonances and weakly bound molecular states of boson-boson and boson-fermion NaK pairs, Phys. Rev. A **93**, 042701 (2016).
[72] B. Gao, E. Tiesinga, C. J. Williams, and P. S. Julienne, Multichannel quantum-defect theory for slow atomic collisions, Phys. Rev. A **72**, 042719 (2005).
[73] F. H. Mies, C. J. Williams, P. S. Julienne, and M. Krauss, Estimating bounds on collisional relaxation rates of Spin-Polarized ^{87}Rb atoms at ultracold temperatures, J. Res. Natl. Inst. Stand. Technol. **101**, 521 (1996).
[74] S. Kotochigova, E. Tiesinga, and P. S. Julienne, Relativistic ab initio treatment of the second-order spin-orbit splitting of the $a\,^3\Sigma_u^+$ potential of rubidium and cesium dimers, Phys. Rev. A **63**, 012517 (2000).
[75] G. F. Gribakin and V. V. Flambaum, Calculation of the scattering length in atomic collisions using the semiclassical approximation, Phys. Rev. A **48**, 546 (1993).
[76] G.-H. Jeung, D. Hagebaum-Reignier, and M. J. Jamieson, Cold collisions of alkali-metal atoms and chromium atoms, J. Phys. B **43**, 235208 (2010).
[77] V. Gurarie, L. Radzihovsky, and A. V. Andreev, Quantum Phase Transitions across a p-Wave Feshbach Resonance, Phys. Rev. Lett. **94**, 230403 (2005).
[78] J. Li, J. Liu, L. Luo, and B. Gao, Three-Body Recombination near a Narrow Feshbach Resonance in ^{6}Li, Phys. Rev. Lett. **120**, 193402 (2018).
[79] V. Barbé, A. Ciamei, B. Pasquiou, L. Reichsöllner, F. Schreck, P. S. Żuchowski, and J. M. Hutson, Observation of Feshbach resonances between alkali and closed-shell atoms, Nat. Phys. **14**, 881 (2018).